

Section 3

**Computational studies including new techniques,
the effect of varying model resolution,
parallel processing**

Influence of horizontal resolution on structure changes of atmospheric stratification in the 2015 Hiroshima heavy rainfall

Teruyuki Kato¹

¹Meteorological Research Institute/Japan Meteorological Agency (Email: tkato@mri-jma.go.jp)

1. Introduction

On 20 August 2014, heavy rainfall exceeding 200 mm 3h⁻¹ occurred in Hiroshima, western Japan. The rainfall was caused by a band-shaped precipitation system (BPS) with a hierarchical structure consisting of convective cells and band-shaped multi-cell clusters that stagnated for 4 hours. The BPS had a back-building type formation, as well as the multi-cell clusters, in which new multi-cell clusters successively formed upstream of the pre-existing ones, and consequently extended northeastward with a width of 20–30 km and a length of about 100 km (Fig. 1a). These features were quantitatively and qualitatively well reproduced by JMA nonhydrostatic model (NHM: Saito et al. 2007) with a horizontal resolution of 250 m (Fig. 1c). Even 2km-resolution NHM (Fig. 1b) also well reproduced horizontal distribution of rainfall, although it cannot simulate a BPS with a hierarchical structure.

In this study, the dependency of horizontal resolution on structure changes of atmospheric stratification is examined focusing on vertical profiles of appearance frequency (AF) of equivalent potential temperature (θ_e) and vertical velocity exceeding some thresholds.

2. Experimental designs

Half-day forecasts with 2km, 1km, 500m and 250m NHMs from 18 JST (=UTC+ 9hs) 19 August 2014 were conducted using initial and boundary conditions produced from hourly available JMA local analyses with a horizontal resolution of 5 km.

Forecast horizontal domain was 1000x800 km for 2km, 1km and 500mNHMs, and 250mNHM with a domain of 412x330 km was run nested within 2kmNHM forecasts. A bulk-type microphysics parameterization scheme in which two moments were treated only for ice hydrometeors was used for precipitation processes. The turbulence closure scheme of Mellor-Yamada-Nakanishi-Niino level-3 (MYNN: Nakanishi and Niino 2006) was used. The other settings including numerical diffusion are the same for all NHMs.

3. Appearance frequency (AF) of θ_e

To understand the change of atmospheric structure caused by convective activities, vertical AF profiles of θ_e exceeding threshold values are examined (Fig. 2). High θ_e exceeding 355 K, found below a 1-km height, is conserved when environmental air is not entrained into lifted air. The AF of such high θ_e is almost the same in 2km and 250mNHMs, although it is very low (0.01–0.001 %) at middle and upper levels. The AF of moderate θ_e (~350 K) found at middle levels is, however, about twice higher in 2kmNHM than in 250mNHM. This could be smaller entrainment of environmental air due to bigger horizontal scales of convection in 2kmNHM. This feature is relaxed in 1kmNHM (Fig. 3a), but AF of high θ_e in 500mNHM (Fig. 3b) considerably decreases compared with the other NHMs. This indicates that high resolution do not always help improve forecasts; 250mNHM is suitable while 500mNHM should be avoided.

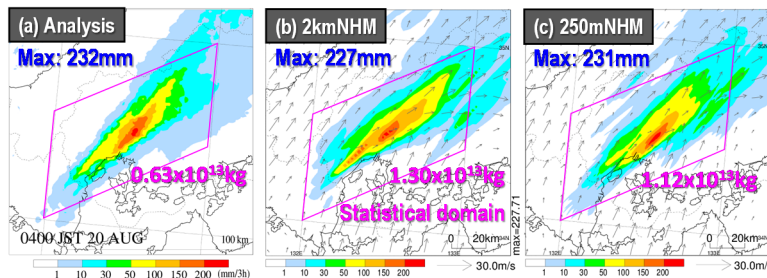


Fig. 1 (a) Distribution of 3-hour accumulated rainfall amounts, estimated using rain gauge and radar observations between 01 and 04 JST 20 August 2014. Same as (a), but (b) 2kmNHM and (c) 250mNHM forecasts. Blue (pink) numbers show the maximum value (total amounts) within pink rectangles.

The change of atmospheric structure from the developing stage to mature stage of convective activities in 250mNHM is shown in Fig. 4. The AF of high θ_e increases by a factor of about 10 (0.001->0.01 %), and that of moderate θ_e is doubled (0.3->0.6 %). These increases are, however, very small for the whole amount. This indicates that even strong

convective activities weakly changes the atmospheric structure, and such a large stabilization as that assumed in the Kain-Fritsch convection parameterization scheme, in which convective available potential energy (CAPE) is reduced up to 15 %, does not occur.

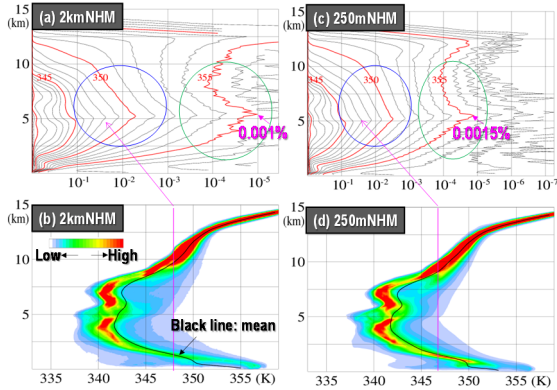


Fig. 2 (a) Vertical AF profiles of θ_e exceeding threshold values, shown by contours with intervals of 1 K, and (b) vertical AF distribution of θ_e within pink rectangles in Fig. 1 between 23 JST 19 and 04 JST 20 August 2014 that are estimated from 1-min interval output of 2kmNHM. (c) and (d) Same as (a) and (b), but for 250mNHM.

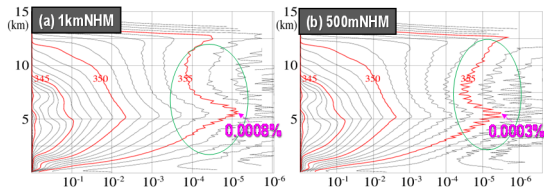


Fig. 3 Same as Fig. 2a, but in (a) 1kmNHM and (b) 500mNHM.

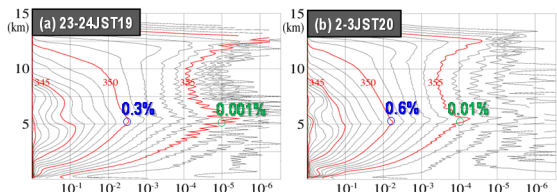


Fig. 4 Same as Fig. 2c, but between (a) 23 and 24 JST 19 (developing stage) (b) 02 and 03 JST 20 August 2014 (mature stage).

4. AF of strong vertical velocity

The maximum updraft and its appearance height are examined related to horizontal resolutions (Fig. 5). The maximum updraft exceeding 18 m s^{-1} is found just below a 10-km height in 2kmNHM. On the other hand, 250mNHM has strong updrafts exceeding 35 m s^{-1} that is about half of an estimated updraft from CAPE ($\sim 2000 \text{ J kg}^{-1}$). The strong updrafts are majorly found a few kilometers below the level of neutral buoyancy (LNB) that is estimated when air with low-level θ_e of 355 K is lifted. Strong updrafts

are also found above the LNB, which indicates that 250mNHM can simulate overshoots. The maximum updraft and its appearance height in 1km and 500mNHMs are illustrated as intermediate features between 2km and 250mNHMs. This shows that a height with the maximum updraft appears lower for lower horizontal resolutions. Noted that AF of moderate updrafts ($\sim 5 \text{ m s}^{-1}$) at middle levels little depends on horizontal resolutions.

The features of downdraft AF are largely different for 2km and 250mNHMs. Strong downdrafts found around a 10-km height in 250mNHM are produced as compensation for strong updrafts. Meanwhile, such strong downdrafts are not found in 2kmNHMs.

Since low-level high θ_e with large CAPE can produce strong updrafts, AF of vertical velocity is examined for $\theta_e > 355 \text{ K}$ (Fig. 6). Vertical motions are accelerated upward with height, as θ_e is almost conserved even in 2kmNHM. Above a 10-km height, AF of $\theta_e > 355 \text{ K}$ (pink line in Fig. 6) decreases rapidly, while strong updrafts remain. This indicates that mixing with environmental field becomes larger, but an examination on detail processes is a future work.

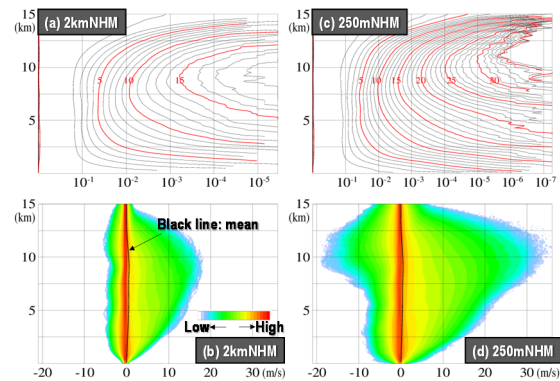


Fig. 5 (a) and (b) Same as Figs. 2a and 2c, but for vertical velocity. (c) and (d) Same as (a) and (b), but in 250mNHM. Contour intervals in (a) and (c) are 1 m s^{-1} .

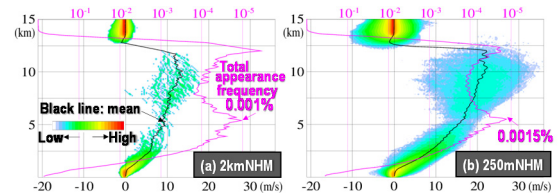


Fig. 6 (a) and (b) Same as Figs. 5b and 5d, but for $\theta_e > 355 \text{ K}$.

References

- Saito, K., J. Ishida, K. Aranami, T. Hara, T. Segawa, M. Nareta, and Y. Honda, 2007: *J. Meteor. Soc. Japan*, **85B**, 271-304.